Photonic Generation of Continuously Tunable Chirped Microwave Waveforms Based on a Temporal Interferometer Incorporating an Optically Pumped Linearly Chirped Fiber Bragg Grating

Ming Li, *Member, IEEE*, and Jianping Yao, *Senior Member, IEEE*

***Abstract*—A novel approach to generating a chirped microwave waveform with continuously tunable chirp rate based on a temporal interferometer incorporating an optically pumped linearly chirped fiber Bragg grating (LCFBG) is proposed and demonstrated. The temporal interferometer is realized using a Mach–Zehnder interferometer (MZI) that incorporates an LCFBG and a dispersion compensating fiber to generate a temporal interference pattern with an instantaneous frequency that is linearly proportional to time. A linearly chirped microwave waveform with its shape that is identical to the temporal interference pattern is generated at the output of a photodetector. The tuning of the chirp rate of the generated waveform is realized by optically pumping the LCFBG that is written in an erbium–ytterbium co-doped fiber with different pumping powers. The key advantage of using optical pumping over external thermal tuning or mechanical tuning to tune the dispersion of the LCFBG is that the dispersion can be tuned at a high speed and controlled remotely. Moreover, the undesirable birefringence effects existing in the mechanical tuning technique can also be avoided. A theoretical analysis is performed that is verified by numerical simulations and an experiment. A linearly chirped microwave waveform with a tunable chirp rate from 79 to 64 GHz/ns by changing the injection current to the pumping laser diode from 0 to 100 mA is generated. The experimental results also show that the central frequency of the generated chirped microwave waveform can be changed by tuning the longitudinal offset of the MZI.**

***Index Terms*—Chirped microwave waveform generation, erbium–ytterbium (Er/Yb) co-doped fiber, fiber Bragg grating (FBG), linearly chirped fiber Bragg grating (LCFBG), temporal interferometry.**

I. Introduction

PHOTONIC generation of chirped microwave waveforms has been a topic of interest recently, which can find many important applications such as modern radar, ultra-fast wired and wireless communications, medical imaging, and modern instrumentation [1]. In a radar system, for example, the range resolution can be improved while maintaining a large detection distance due to the use of a chirped microwave waveform to achieve pulse compression [2]. Although a chirped microwave waveform can be generated in the electrical domain, the central frequency and bandwidth are usually small due to the limited sampling rate of the currently available digital electronics. For many applications, however, a chirped microwave waveform with a central frequency up to tens or even hundreds of gigahertz and a bandwidth up to tens of gigahertz is required [3]. The key advantages of using photonic techniques for chirped microwave waveform generation are the ultrafast speed and broad bandwidth that can meet the high-frequency and broad-bandwidth requirements. Numerous photonically assisted techniques have been proposed recently to generate chirped microwave waveforms based on either free-space optics or fiber optics [4]–[7]. Compared with free-space optics, waveform generation based on pure fiber optics offers advantages, such as smaller size, lower loss, better stability, and higher potential for integration.

Optical spectral-shaping and wavelength-to-time (SS-WTT) mapping is an important technique that has been recently employed to generate chirped microwave waveforms [6], [7]. In an SS-WTT mapping system, a chirped microwave waveform is generated by shaping the spectrum of an ultrashort optical pulse using a spectral filter with an increasing or decreasing free spectral range (FSR), followed by wavelength-to-time mapping in a dispersive element [6]. Due to the linear wavelength-to-time mapping, a chirped microwave waveform with a shape that is a scaled version of the shaped spectrum is generated [6]. The key device in an SS-WTT system for a chirped microwave waveform generation is the spectral filter, which should have a spectral response with an increasing or decreasing FSR. Such a spectral filter can be implemented using two superimposed linearly chirped fiber Bragg gratings (LCFBGs) with a spatial offset between the two LCFBGs [8], or a spatially discrete fiber Bragg grating (FBG) [9]. The major limitation of these techniques is that the generated waveform is not tunable since the spectral response of the spectral filter is hard to be tuned once the filter is constructed. Recently, we demonstrated a chirped microwave waveform generator using a spectral filter that consists of a Sagnac-loop mirror incorporating an LCFBG [10]. The center frequency and the sign of the chirp rate could be tunable, but the absolute value of the chirp rate is kept constant. Recently, a photonic approach to generating a high-frequency microwave pulse with tunable chirp rate based on nonlinear wavelength-to-time

Manuscript received March 15, 2011; revised August 06, 2011; accepted August 29, 2011. Date of publication October 26, 2011; date of current version December 14, 2011. This work was supported by the Natural Sciences and Engineering Research Council of Canada (NSERC). This paper is an expanded paper from the IEEE International Microwave Symposium, Baltimore, MD, June 5–10, 2011.

The authors are with the Microwave Photonics Research Laboratory, School of Electrical Engineering and Computer Science, University of Ottawa, Ottawa, ON, Canada K1N 6N5 (e-mail: jpyao@site.uOttawa.ca).

Color versions of one or more of the figures in this paper are available online at http://ieeexplore.ieee.org.

Digital Object Identifier 10.1109/TMTT.2011.2169078

mapping using a dispersive fiber with the third-order dispersion was proposed. The major limitation of this technique is that the central frequency of the generated microwave pulse is largely changed when its chirp rate is tuned [11].

In this paper, a novel approach to generating a chirped microwave waveform with continuously tunable chirp rate based on temporal interferometry is proposed and experimentally demonstrated. The chirp rate and central frequency of the generated microwave waveform can be tuned separately. The proposed chirped microwave waveform generation system is similar to the SS-WTT mapping system reported in [10], but the key difference is that an optically pumped LCFBG is employed in a Mach–Zehnder interferometer (MZI) serving as the spectral filter. The spectral response of the MZI has an increasing or decreasing FSR, which is tunable by pumping the LCFBG. After wavelength-to-time mapping in a dispersion compensating fiber (DCF), a temporal interference pattern with an instantaneous frequency that is linearly increasing with time is generated. The detection of the temporal interference pattern at a photodetector would generate a linearly chirped microwave waveform. The optically pumped LCFBG is written in an erbium–ytterbium (Er/Yb) co-doped fiber. By pumping the LCFBG with different pumping power, the group-delay response will be changed, leading to the change of the FSR of the spectral response. The key advantage of using optical tuning over an external thermal [12] or mechanical tuning [13] to tune the dispersion of the LCFBG is that the dispersion can be tuned at a high speed and controlled remotely. In addition, the undesirable birefringence effects existing in the mechanical tuning technique can also be avoided. Some preliminary results have been presented in [14]. In this paper, the proposed system is investigated in detail. A theoretical analysis is presented, which is verified by numerical simulations and an experiment. A linearly chirped microwave waveform with a tunable chirp rate from 79 to 64 GHz/ns by changing the injection current to the pumping laser diode from 0 to 100 mA is experimentally demonstrated. The tuning of the central frequency of the generated chirped microwave waveform by tuning the longitudinal offset of the MZI is also experimentally demonstrated.

II. Principle

The fundamental principle of the proposed technique is illustrated in Fig. 1. An ultrashort transform-limited optical pulse emitted from a mode-locked laser (MLL) is directed into the two arms of an MZI. The optical pulse passing through the upper arm (arm 1) is time stretched by the LCFBG in the arm and then the DCF at the output of the MZI. The optical pulse directed into the lower arm (arm 2) is only experiencing a time delay in the arm and then stretched by the DCF. The two time-stretched optical pulses are combined to generate a temporal interference pattern with an increasing or decreasing FSR. Using an opto-electronic converter, the temporal interference pattern is converted to a chirped microwave waveform.

The key component in the system is the LCFBG, which is inscribed in an Er/Yb co-doped fiber. When the LCFBG is optically pumped from the red end, i.e., the end with a longest period, the temperature at the red end would increase, which would

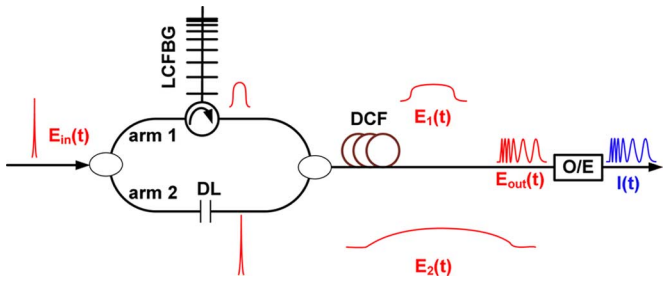

Fig. 1. Temporal interferometer for a chirped microwave waveform generation. An LCFBG is incorporated in arm 1 of the interferometer, and a DCF is used to stretch the two pulse from the interferometer. Linearly chirped fiber Bragg grating: LCFBG, delay line: DL, dispersion compensating fiber: DCF, opto-electronic converter: O/E.

broaden the reflection spectrum as a consequence of the increase in the core refractive index [15]. Therefore, the absolute value of the dispersion of the LCFBG is decreased due to the optical pumping. By tuning the injection current to the pumping laser diode, the dispersion of the LCFBG can be continuously tuned [16].

The transform-limited Gaussian pulse from the MLL can be expressed as $g(t) = \exp(-t^2/\tau_0^2)$, where τ_0 is the half pulsewidth at $1/e$ maximum. Its Fourier transform is given by $G(\omega) = \sqrt{\pi}\tau_0 \exp(-\tau_0^2\omega^2/4)$, where ω denotes the angular frequency. The transfer functions of the LCFBG and the DCF are given, respectively, by $H_{\rm FBG}(\omega) = |r(\omega)|\exp(j\ddot{\Phi}_{\rm FBG}\omega^2/2)$ and $H_{\rm DCF}(\omega) = \exp(j\ddot{\Phi}_{\rm DCF}\omega^2/2)$, where $\ddot{\Phi}_{\rm FBG}$ and $\ddot{\Phi}_{\rm DCF}$ are the group velocity dispersion (GVD) of the LCFBG and the DCF, respectively, and $|r(\omega)|$ denotes the magnitude response of the LCFBG in reflection.

In arm 1, the ultrashort optical pulse is temporally stretched and spectrally dispersed by passing through the LCFBG. Meanwhile, the optical pulse is also spectrally filtered by the LCFBG. The temporally stretched and spectrally filtered pulse is further stretched by the DCF. When the condition $|\tau_0^2/2\ddot{\Phi}_{\rm FD}| \ll 1$ is satisfied, where $\ddot{\Phi}_{\rm FD} = \ddot{\Phi}_{\rm FBG} + \ddot{\Phi}_{\rm DCF}$, the input optical pulse $g(t)$ is approximately real-time Fourier transformed [17]. As shown in Fig. 1, the electrical field $E_1(t)$ of the optical signal from arm 1 at the output of the DCF is given by

$$E_1(t) = C_1 \times |r(\omega)| \times \exp\left[j\frac{\ddot{\Phi}_{\rm FD}}{2}\omega^2\right] \times G(\omega)\Big|_{\omega=\frac{t_{\rm FD}}{\ddot{\Phi}_{\rm FD}}} \quad (1)$$

where $t_{\rm FD} = t - \dot{\Phi}_1$ is the time measured relative to the average time delay where $\dot{\Phi}_1 = \dot{\Phi}_{\rm arm1} + \dot{\Phi}_{\rm DCF}$, $\dot{\Phi}_{\rm arm1}$ and $\dot{\Phi}_{\rm DCF}$ denote the average time delays of the light, in arm 1 of the MZI and the DCF, respectively, and C_1 is a time-independent constant, which represents the attenuation in arm 1.

In arm 2, the input optical pulse is first time delayed by an optical fiber delay line. The time-delayed optical pulse is then temporally stretched and spectrally dispersed by passing through the DCF. When the condition $|\tau_0^2/2\ddot{\Phi}_{\rm DCF}| \ll 1$ is satisfied,

the electrical field $E_2(t)$ of the optical signal from arm 2 at the output of the DCF can be expressed by

$$E_2(t) = C_2 \times \exp\left[j\frac{\ddot{\Phi}_{\rm DCF}}{2}\omega^2\right] \times G(\omega)\Big|_{\omega=\frac{t_{\rm DCF}}{\ddot{\Phi}_{\rm DCF}}} \tag{2}$$

where $t_{\rm DCF} = t - \dot{\Phi}_2$ is the time measured relative to the average time delay where $\dot{\Phi}_2 = \dot{\Phi}_{\rm arm2} + \dot{\Phi}_{\rm DCF}$, $\dot{\Phi}_{\rm arm2}$ and $\dot{\Phi}_{\rm DCF}$ denote the average time delays of the light in arm 2 of the MZI and the DCF, respectively, and C_2 is a time-independent constant.

The two optical pulses from the two arms are combined at the output the DCF, where the electrical field $E_{\rm out}(t)$ can be written as

$$E_{\rm out}(t) = E_1(t) + E_2(t). \tag{3}$$

If the optical signal at the output of the DCF is applied to a photodetector, we have the output current, given by

$$\begin{aligned} I &= \Re E_{\rm out}(t) \times \overline{E_{\rm out}(t)} \\ &\propto \left[C_1 \times \left| r\left(\frac{t_{\rm FD}}{\ddot{\Phi}_{\rm FD}}\right)\right| \times G\left(\frac{t_{\rm FD}}{\ddot{\Phi}_{\rm FD}}\right)\right]^2 \\ &\quad + \left[C_2 \times G\left(\frac{t_{\rm DCF}}{\ddot{\Phi}_{\rm DCF}}\right)\right]^2 \\ &\quad + C_1 \times C_2 \times \left| r\left(\frac{t_{\rm FD}}{\ddot{\Phi}_{\rm FD}}\right)\right| \times G\left(\frac{t_{\rm FD}}{\ddot{\Phi}_{\rm FD}}\right) \times G\left(\frac{t_{\rm DCF}}{\ddot{\Phi}_{\rm DCF}}\right) \\ &\quad \times \left[2\cos\left(\frac{t_{\rm DCF}^2}{2\ddot{\Phi}_{\rm DCF}} - \frac{t_{\rm FD}^2}{2\ddot{\Phi}_{\rm FD}}\right)\right] \end{aligned} \tag{4}$$

where $\Re$ is the photo responsivity of the photodetector. Note that, according to the basic principle of an MZI, when $C_1 = C_2$ is satisfied, the fringe visibility of the generated chirped microwave waveform is maximized. In addition, since the bandwidth of the LCFBG is much smaller than the bandwidth of the ultrashort optical pulse, the pulsewidth of the generated chirped microwave waveform is mainly determined by the term $|r((t_{\rm FD})/(\ddot{\Phi}_{\rm FD}))|$, which represents the wavelength-to-time mapping of the magnitude response of the LCFBG. It can be seen from (4) that when the bandwidth of the input pulse is larger than that of the LCFBG, the time duration of the generated microwave waveform is determined by the bandwidth of the LCFBG. On the other hand, when the bandwidth of the input pulse is smaller than that of the LCFBG, the time duration of the generated microwave waveform is determined by the bandwidth of the input pulse.

It can also be seen from (4) that the chirped microwave waveform is mainly determined by the term $\cos((t_{\rm DCF}^2)/(2\ddot{\Phi}_{\rm DCF}) - (t_{\rm FD}^2)/(2\ddot{\Phi}_{\rm FD}))$. Thus, the phase $\phi_{\rm RF}$ of the chirped microwave waveform is given by

$$\phi_{\rm RF} = \frac{t_{\rm DCF}^2}{2\ddot{\Phi}_{\rm DCF}} - \frac{t_{\rm FD}^2}{2\ddot{\Phi}_{\rm FD}} = \frac{\left(t - \dot{\Phi}_2\right)^2}{2\ddot{\Phi}_{\rm DCF}} - \frac{\left(t - \dot{\Phi}_1\right)^2}{2\ddot{\Phi}_{\rm FD}}. \tag{5}$$

From (5), the instantaneous carrier frequency of the generated chirped microwave waveform $f_{\rm RF}$ can be

$$\begin{aligned} f_{\rm RF} &= \frac{1}{2\pi}\frac{d\phi_{\rm RF}}{dt} \\ &= \frac{1}{2\pi}\left(\frac{\ddot{\Phi}_{\rm FD} - \ddot{\Phi}_{\rm DCF}}{\ddot{\Phi}_{\rm FD}\ddot{\Phi}_{\rm DCF}}\right)t - \frac{1}{2\pi}\left(\frac{\dot{\Phi}_2\ddot{\Phi}_{\rm FD} - \ddot{\Phi}_{\rm DCF}\dot{\Phi}_1}{\ddot{\Phi}_{\rm FD}\ddot{\Phi}_{\rm DCF}}\right). \end{aligned} \tag{6}$$

It can be seen from (6) that the instantaneous microwave carrier frequency of the generated microwave waveform is linearly proportional to time, therefore it is linearly chirped. In addition, the term $-(1)/(2\pi)((\dot{\Phi}_2\ddot{\Phi}_{\rm FD} - \ddot{\Phi}_{\rm DCF}\dot{\Phi}_1)/(\ddot{\Phi}_{\rm FD}\ddot{\Phi}_{\rm DCF}))$ denotes the central frequency f_0 of the chirped microwave waveform, which can be rewritten as

$$\begin{aligned} f_0 = &-\frac{1}{2\pi}\left(\frac{\ddot{\Phi}_{\rm DCF}(\dot{\Phi}_{\rm arm1} - \dot{\Phi}_{\rm arm2})}{\ddot{\Phi}_{\rm FD}\ddot{\Phi}_{\rm DCF}}\right) \\ &+\frac{1}{2\pi}\left(\frac{\ddot{\Phi}_{\rm FBG}(\dot{\Phi}_{\rm arm2} + \dot{\Phi}_{\rm DCF})}{\ddot{\Phi}_{\rm FD}\ddot{\Phi}_{\rm DCF}}\right). \end{aligned} \tag{7}$$

Since the second term at the right-hand side of (7) represents an extremely high-frequency term that cannot be detected by a photodetector in general and the frequency of a microwave waveform should be kept positive, we have

$$f_0 = \frac{1}{2\pi}\left|\frac{(\dot{\Phi}_{\rm arm1} - \dot{\Phi}_{\rm arm2})}{\ddot{\Phi}_{\rm FD}}\right|. \tag{8}$$

From (8), it can be seen that by tuning the average time-delay difference between the two interference arms using a tunable delay line, the central frequency of the generated chirped microwave waveform can be changed.

In addition, when the sign of the average time-delay difference between arm 1 and arm 2 is reversed, the sign of the chirp rate of the generated microwave waveform is also changed. Based on (6), the chirp rate of the generated microwave waveform can be written as

$$\begin{aligned} {\rm CR} &= \frac{df_{\rm RF}}{dt} \\ &= \frac{1}{2\pi}{\rm sgn}(\dot{\Phi}_{\rm arm1} - \dot{\Phi}_{\rm arm2})\left(\frac{1}{\left(1 + \frac{\ddot{\Phi}_{\rm DCF}}{\ddot{\Phi}_{\rm FBG}}\right)\ddot{\Phi}_{\rm DCF}}\right). \end{aligned} \tag{9}$$

From (9), it is obvious that the chirp rate can be continuously tuned by changing the dispersion of the LCFBG. Therefore, by appropriately designing the longitudinal offset and the dispersion of the LCFBG, a linearly chirped microwave waveform with a high central frequency and a large and continuously tunable chirp rate can be generated.

III. Numerical Simulations

Numerical simulations are performed to verify the theoretical analysis and to demonstrate the photonic generation of a chirped microwave waveform with a continuously tunable chirp rate by

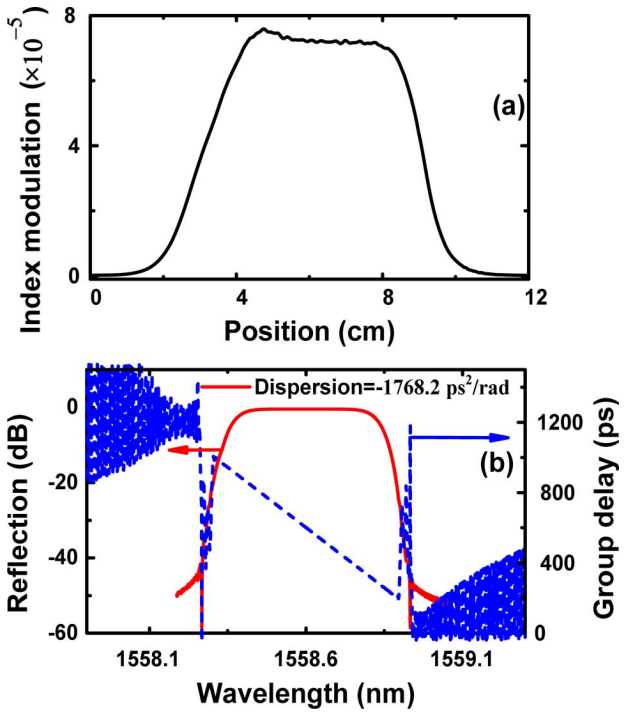

Fig. 2. (a) Index modulation of the designed LCFBG and (b) its reflection and group-delay spectra.

changing the pumping power to the LCFBG and a tunable central frequency by changing the time delay via the tunable delay line. In the simulations, a transform-limited ultrashort Gaussian pulse with a half pulsewidth at $1/e$ maximum of 202.35 fs and with a central wavelength λ_c of 1558.6 nm is used as the input optical pulse. A DCF with a dispersion value of 1210.1 ps^2/rad is employed in the simulation.

A. *Effect of the Longitudinal Offset*

In the first simulation, we study the tuning of the central frequency of the chirped waveform by tuning the optical path difference. An LCFBG is designed by using the discrete layer peeling algorithm [18]. Fig. 2(a) shows the index modulation profile of the designed LCFBG with a length of 12 cm. As shown in Fig. 2(b), the LCFBG has a bandwidth of 0.5 nm and a dispersion value of 1768.2 ps^2/rad.

For a light wave with a central wavelength λ_c that is identical to the central wavelength of the LCFBG directed into the MZI, the optical path difference between the two arms can be written as $\Delta L = L_{\rm arm1}(\lambda_c) - L_{\rm arm2}(\lambda_c)$, where $L_{\rm arm1}$ and $L_{\rm arm2}$ are the optical paths of the light passing through arm 1 and arm 2, respectively. Different values of the longitudinal offset are chosen by tuning the tunable delay line in the MZI, leading to a generated chirped microwave waveform with a symmetrical, monotonically increasing, or monotonically decreasing instantaneous microwave frequency, as shown in Fig. 3(a)–(c). The chirp rates of the generated microwave waveforms are also shown in Fig. 3(a)–(c), which match well with the theoretical prediction (i.e., 78.08 GHz/ns) given by (9). It can be concluded that the central frequency of the generated microwave waveform can be tuned by changing the longitudinal offset. Note that the

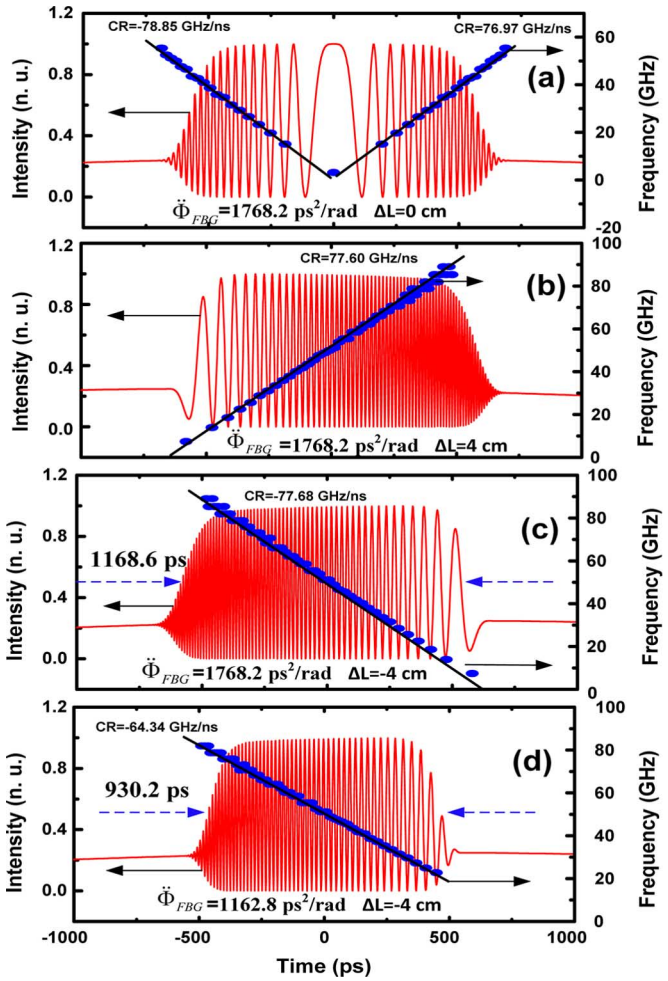

Fig. 3. Simulated output microwave waveforms with different longitudinal offset ΔL between the two arms of the MZI and different value of dispersion $\ddot{\Phi}_{\rm FBG}$ of the LCFBG. (a) $\ddot{\Phi}_{\rm FBG} = 1768.2$ ps^2/rad, $\Delta L = 0$ cm. (b) $\ddot{\Phi}_{\rm FBG} = 1768.2$ ps^2/rad, $\Delta L = 4$ cm. (c) $\ddot{\Phi}_{\rm FBG} = 1768.2$ ps^2/rad, $\Delta L = -4$ cm. (d) $\ddot{\Phi}_{\rm FBG} = 1162.8$ ps^2/rad, $\Delta L = -4$ cm.

simulations are implemented based on the equations presented in Section II along with the designed grating shown in Fig. 2.

B. *Influence of the Dispersion of the LCFBG*

We then study the change of the dispersion value of the LCFBG on the chirp rate of the generated waveform. A second LCFBG with a bandwidth of 0.5 nm and a value of dispersion of 1162.8 ps^2/rad is designed based on the discrete layer peeling algorithm. As shown in Fig. 3(d), when the dispersion value of the LCFBG is changed from 1768.2 to 1162.8 ps^2/rad, the chirp rate of the generated chirped microwave waveform is changed from -77.68 to -64.34 GHz/ns. The theoretical prediction of the chirped microwave waveform by (9) is 65.17 GHz/ns, which agrees well with the simulated result. It is worth noting that the chirp rate can be further decreased based on an LCFBG with a smaller value of dispersion. In addition, the dispersion can be increased by optically pumping the LCFBG from the blue end (i.e., the shorter wavelength end), the chirp rate can then be increased.

As shown in Fig. 3(c), the dispersion $\ddot{\Phi}_{\rm FD}$ is equal to 2978.3 ps^2/rad and the LCFBG has a bandwidth of 0.5 nm.

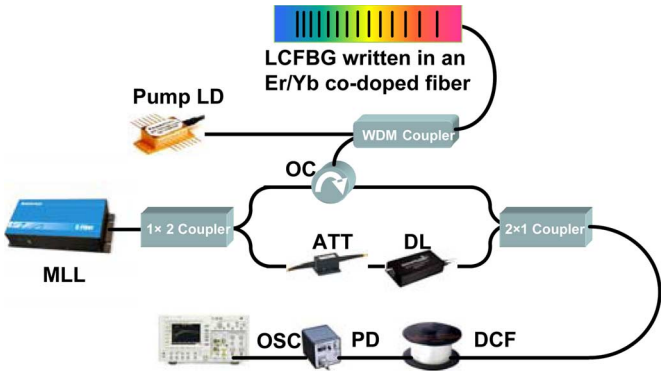

Fig. 4. Experimental setup of a chirped pulse generation system. Linearly chirped fiber Bragg grating: LCFBG, dispersion compensating fiber: DCF, opto-electronic converter: O/E, mode-locked laser: MLL, optical circulator: OC, laser diode: LD, wavelength division multiplexing: WDM, attenuator: ATT, delay line: DL, photodetector: PD, oscilloscope: OSC.

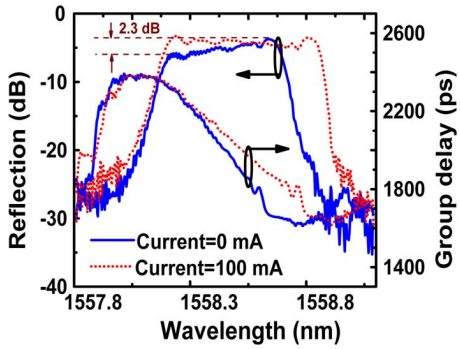

Fig. 5. Reflection and group-delay responses of the LCFBG inscribed in an Er/Yb co-doped fiber with (dotted line) and without (solid line) optical pumping.

From (4), the calculated temporal width of the generated chirped microwave waveform is equal to 1163.4 ps, which agrees well with the numerical result of 1168.6 ps. From Fig. 3(d), the temporal width becomes 930.2 ps when the value of dispersion $\ddot{\Phi}_{\mathrm{FD}}$ is decreased to 2372.9 ps^2/rad. The calculated result is 926.9 ps. Again, a good agreement is achieved between the numerical and theoretical results.

From the simulation results shown in Fig. 3, it can be concluded that a linearly chirped microwave waveform with a high central frequency and a large and continuously tunable chirp rate can be generated by tuning the dispersion of the LCFBG. In addition, the central wavelength of the generated chirped microwave waveform can be changed by tuning the longitudinal offset of the MZI.

IV. Experiment

Fig. 4 shows the experimental setup of the chirped microwave waveform generation system based on an MZI incorporating an LCFBG written in an Er/Yb co-doped fiber. The MZI is constructed using two 3-dB 1×2 optical couplers. An LCFBG inscribed in an Er/Yb co-doped fiber is incorporated into the upper arm (arm 1) of the MZI via an optical circulator (OC). A laser diode with a lasing wavelength of 980 nm is used to pump the LCFBG via a wavelength division multiplexing (WDM) coupler. The group-delay response of the LCFBG can be tuned by optically pumping the LCFBG with different pumping power [16]. A tunable delay line located in the lower arm (arm 2) is used to tune the time-delay difference between the two arms. A tunable optical attenuator is used to adjust the attenuations between the two arms, to adjust and maximize the fringe visibility of the interference pattern at the output of the MZI.

In the experiment, an ultrashort pulse with a half pulsewidth at $1/e$ maximum of 202.35 fs, a full-width at half-maximum (FWHM) bandwidth of 8 nm, and a central wavelength of 1558.6 nm generated by a MLL is sent to the MZI. The pulse train from the MLL has a repetition rate of 48.6 MHz. Note that the repetition rate cannot be too high to avoid the overlapping of two neighboring waveforms at the output of the generation system. The LCFBG has a length of $\sim$8 cm, which is fabricated with a UV beam-scanning technique using a linearly chirped phase mask with a chirp rate of 0.09 nm/cm. The fiber used to fabricate the LCFBG is a hydrogen-loaded Er/Yb co-doped fiber. The dispersion value of the DCF connected after the MZI is about 1210.1 ps^2/rad. A chirped microwave waveform with a shape that is identical to the temporal interference pattern of the MZI is then generated at the output of a high-speed photodetector. The waveform is observed by a high-speed sampling oscilloscope (OSC, Agilent 86116A).

Fig. 5 shows the reflection and group-delay responses of the fabricated LCFBG with a central wavelength of 1558.5 nm. When the injection current of the pumping laser diode is 0 mA, the absolute value of the dispersion of the LCFBG is about 1768.2 ps^2/rad. When the LCFBG is pumped from the red end by a 980-nm laser diode with an injection current of 100 mA (i.e., 101 mW), the absolute value of the dispersion is decreased to about 1162.8 ps^2/rad. On the other hand, as mentioned in Section II, in an Er/Yb co-doped fiber, the core refractive index would change as a consequence of the variation of the pumping power. When the LCFBG is pumped from the red end, as shown in Fig. 5, the wavelength reflected at the red end is increased to broaden the bandwidth of the reflection spectrum.

In the first experiment, the longitudinal offset is tuned to be about 4 cm, which is large enough to shift the waveform with a zero instantaneous microwave carrier frequency out of the main lobe. The generated chirped microwave waveforms are shown in Fig. 6(a) and (b). The instantaneous frequencies of the generated microwave waveforms are also shown in Fig. 6(a) and (b) (as dotted lines), which are obtained by calculating the reciprocal of the spacing of adjacent peaks. Linear curve fitting for the measured instantaneous frequencies is also performed, and shown in Fig. 6(a) and (b) (as dashed lines). For both cases in which the LCFBG is not or is pumped, a linearly chirped microwave waveform is generated, but with different chirp rates. Without pumping, the instantaneous frequency is linearly decreasing from 55 to 11 GHz within the waveform mainlobe, with an equivalent frequency chirp rate of 79 GHz/ns, which agrees well with the theoretical result of 78.08 GHz/ns. According to the experimental results, a time-bandwidth product (TBWP) of 24.5 is achieved for the waveform. In Fig. 6(a), the central frequency of the generated microwave waveform is about 39.54 GHz, which again agrees well with the theoretical result of 44.8 GHz by (8). When the LCFBG is pumped by the 980-nm laser diode with an injection current of 100 mA, a

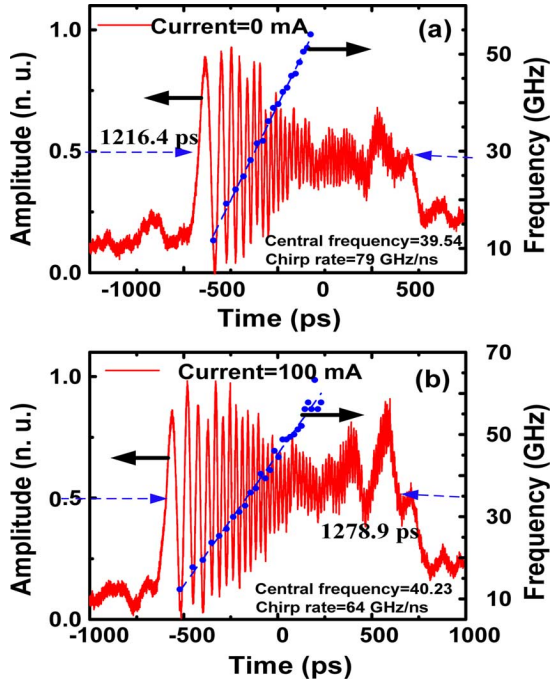

Fig. 6. Experimental result ($\Delta L = 4$ cm): the generated linearly chirped microwave waveform [solid + red line (in online version)] and the instantaneous frequency [blue dots (in online version)]. (a) Without pumping. (b) With optical pumping. Dashed line: linear curve fitting of the instantaneous frequency.

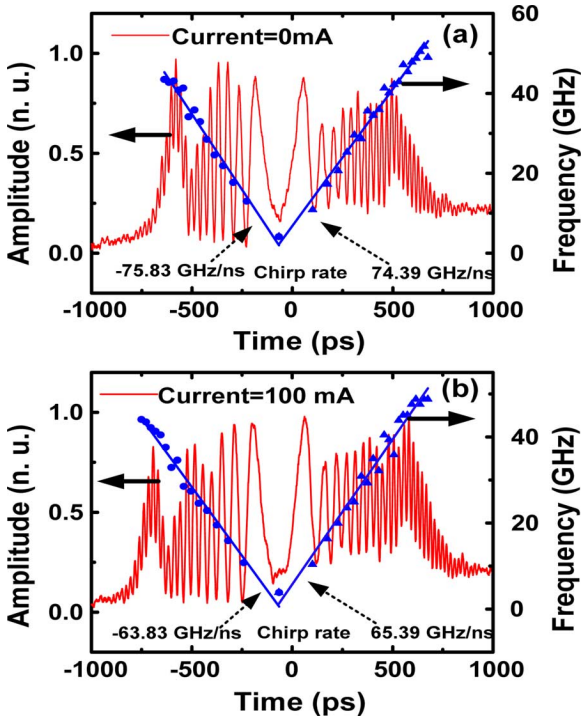

Fig. 7. Experimental results ($\Delta L = 0$ cm): the generated linearly chirped microwave waveform [solid+red line (in online version)] and the instantaneous frequency [blue dots (in online version)]. (a) Without pumping. (b) With optical pumping. Dashed line: linear curve fitting of the instantaneous frequency.

chirped microwave waveform with a chirp rate of 64 GHz/ns is generated. Again, a good agreement between the experimental and theoretical results is reached. The instantaneous frequency is linearly decreasing from 65 to 11 GHz within the waveform mainlobe. A TBWP of 45.56 is achieved.

As shown in Fig. 5, when the injection current of the pumping laser diode is 0 mA, the dispersion $\ddot{\Phi}_{\mathrm{FD}}$ is equal to 2978.3 ps^2/rad and the LCFBG has a bandwidth of 0.52 nm. From (4), the calculated temporal width of the generated chirped microwave waveform is equal to 1209.9 ps, which agrees well with the experimental result of 1216.4 ps, as is shown in Fig. 6(a). From Fig. 6(b), the temporal width becomes 1278.9 ps when the dispersion $\ddot{\Phi}_{\mathrm{FD}}$ is decreased to 2372.9 ps^2/rad and the bandwidth of the LCFBG is equal to 0.69 nm. The calculated result is 1279.1 ps. Again, an excellent agreement is achieved between the experimental and theoretical results.

In the second experiment, the longitudinal offset between the two arms of the MZI is tuned to be about zero. As shown in Fig. 7, the generated chirped microwave waveform has a symmetrical and linearly changing microwave carrier frequency, which agrees well with the simulated results. Moreover, the resulted chirp rate of the microwave waveform with and without optical pumping again agrees well with the theoretical results.

Note that the chirp rate can be further decreased by increasing the injection current to the pump laser diode. It is worth noting that the amplitude of the chirped microwave waveform is not constant within the mainlobe, instead, the amplitude is decreasing when the microwave frequency is increasing, as shown in Fig. 6(a) and (b). The main reason that leads to the amplitude decrease is due to the limited bandwidth (i.e., 53 GHz) of the photodetector. For the waveforms shown in Fig. 7, since the carrier frequency is always smaller than 50 GHz in the main lobe, the amplitude of the chirped microwave waveform is almost constant in the main lobe. If a photodetector with a broader bandwidth is employed, we should be able to generate a chirped microwave waveform with more constant amplitude in Fig. 6.

Note also that the stability of the generated chirped microwave waveforms is limited due to the use of an MZI structure, which is sensitive to environmental changes. A simple solution is to package the system with temperature and variation control. An ultimate solution is to replace the fiber-based MZI by an integrated MZI incorporating a linearly chirped waveguide grating inscribed in a doped waveguide.

V. Conclusion

We have proposed and demonstrated a novel method to generate a chirped microwave waveform with a continuously tunable chirp rate based on a temporal interferometer incorporating an optically pumped LCFBG. The temporal interferometer has an MZI structure incorporating an optically pumped LCFBG written in an Er/Yb co-doped fiber. A linearly chirped microwave waveform was generated at the output of the photodetector. By pumping the LCFBG, the interference pattern would have an increasing or decreasing FSR, which would lead to the change of the chirp rate of the chirped microwave waveform. An LCFBG written in an Er/Yb co-doped fiber was fabricated. The incorporation of the LCFBG in the proposed chirped microwave waveform generation system to

generate a chirped microwave waveform was demonstrated. The experimental results showed that a chirped microwave waveform with a tunable chirp rate from 79 to 64 GHz/ns could be generated by changing the injection current to the pumping laser diode from 0 to 100 mA. The central frequency of the generated chirped microwave waveform could be changed by tuning the longitudinal offset of the MZI, which was also verified by the experiments.

REFERENCES

[1] A. M. Weiner, "Femtosecond pulse shaping using spatial light modulators," *Rev. Sci. Instrum.*, vol. 71, no. 5, pp. 1929–1960, May 2000.

[2] C. Wang and J. P. Yao, "Chirped microwave pulse compression using a photonic microwave filter with a nonlinear phase response," *IEEE Trans. Microw. Theory Tech.*, vol. 57, no. 2, pp. 496–504, Feb. 2009.

[3] A. W. Rihaczek, *Principles of High-Resolution Radar*. Norwood, MA: Artech House, 1996.

[4] J. Chou, Y. Han, and B. Jalali, "Adaptive RF-photonic arbitrary waveform generator," *IEEE Photon. Technol. Lett.*, vol. 15, no. 4, pp. 581–583, Apr. 2003.

[5] J. D. McKinney, D. E. Leaird, and A. M. Weiner, "Millimeter-wave arbitrary waveform generation with a direct space-to-time pulse shaper," *Opt. Lett.*, vol. 27, no. 15, pp. 1345–1347, Aug. 2002.

[6] H. Chi and J. P. Yao, "All-fiber chirped microwave pulse generation based on spectral shaping and wavelength-to-time conversion," *IEEE Trans. Microw. Theory Tech.*, vol. 55, no. 9, pp. 1958–1963, Sep. 2007.

[7] C. Wang and J. P. Yao, "Photonic generation of chirped millimeter-wave pulses based on nonlinear frequency-to-time mapping in a nonlinearly chirped fiber Bragg grating," *IEEE Trans. Microw. Theory Tech.*, vol. 56, no. 2, pp. 542–553, Feb. 2008.

[8] C. Wang and J. P. Yao, "Photonic generation of chirped microwave pulses using superimposed chirped fiber Bragg gratings," *IEEE Photon. Technol. Lett.*, vol. 20, no. 11, pp. 882–884, Jun. 2008.

[9] C. Wang and J. P. Yao, "Large time-bandwidth product microwave arbitrary waveform generation using a spatially discrete chirped fiber Bragg grating," *J. Lightw. Technol.*, vol. 28, no. 11, pp. 1652–1660, Jun. 2010.

[10] C. Wang and J. P. Yao, "Chirped microwave pulse generation based on optical spectral shaping and wavelength-to-time mapping using a Sagnac-loop mirror incorporating a chirped fiber Bragg grating," *J. Lightw. Technol.*, vol. 27, no. 16, pp. 3336–3341, Aug. 2009.

[11] R. Ashrafi, Y. Park, and J. Azana, "Fiber-based photonic generation of high-frequency microwave pulses with reconfigurable linear chirp control," *IEEE Trans. Microw. Theory Tech.*, vol. 58, no. 11, pp. 3312–3319, Nov. 2010.

[12] J. Lauzon, S. Thibault, J. Martin, and F. Ouellette, "Implementation and characterization of fiber Bragg gratings linearly chirped by a temperature gradient," *Opt. Lett.*, vol. 19, no. 23, pp. 2027–2029, Dec. 1994.

[13] Y. Liu, J. P. Yao, X. Dong, and J. Yang, "Tunable chirping of a fibre Bragg grating without center wavelength shift using simply supported beam," *Opt. Eng.*, vol. 41, no. 4, pp. 740–741, Apr. 2002.

[14] M. Li, W. Liu, and J. P. Yao, "Continuously tunable chirped microwave pulse generation using an optically pumped linearly chirped fiber Bragg grating," in *IEEE MTT-S Int. Microw. Symp. Dig.*, Baltimore, MD, Jun. 2011, Paper WEPL-1.

[15] M. K. Davis, M. J. Digonnet, and R. Pantell, "Thermal effects in doped fibers," *J. Lightw. Technol.*, vol. 16, no. 6, pp. 1013–1023, Jun. 2003.

[16] H. Shahoei, M. Li, and J. P. Yao, "Continuously tunable time delay using an optically pumped linearly chirped fiber Bragg grating," *J. Lightw. Technol.*, vol. 29, no. 10, pp. 1465–1472, May 2011.

[17] M. A. Muriel, J. Azana, and A. Carballar, "Real-time Fourier transformer based on fiber gratings," *Opt. Lett.*, vol. 24, no. 1, pp. 1–3, Jan. 1999.

[18] J. Skaar, L. Wang, and T. Erdogen, "On the synthesis of fiber Bragg grating by layer peeling," *IEEE J. Quantum. Electron.*, vol. 37, no. 2, pp. 165–173, Feb. 2001.

Ming Li (S'08–M'09) received the Ph.D. degree in electrical and electronics engineering from the University of Shizuoka, Hamamatsu, Japan, in 2009.

In April 2009, he joined the Microwave Photonics Research Laboratory, School of Electrical Engineering and Computer Science, University of Ottawa, Ottawa, ON, Canada, as a Postdoctoral Research Fellow. His current research interests include advanced FBGs and the applications to microwave photonics, ultrafast optical signal processing, arbitrary waveform generation, and optical microelectromchanical systems (MEMS) sensing.

Jianping Yao (M'99–SM'01) received the Ph.D. degree in electrical engineering from the Université de Toulon, Toulon, France, in 1997.

In 2001, he joined the School of Electrical Engineering and Computer Science, University of Ottawa, Ottawa, ON, Canada, where he is currently a Professor, Director of the Microwave Photonics Research Laboratory, and Director of the Ottawa–Carleton Institute for Electrical and Computer Engineering. From 1999 to 2001, he held a faculty position with the School of Electrical and Electronic Engineering, Nanyang Technological University, Singapore. He holds a Yongqian Endowed Visiting Chair Professorship with Zhejiang University, Hangzhou, China. In 2005, he spent three months as an Invited Professor with the Institut National Polytechnique de Grenoble, Grenoble, France. He was named University Research Chair in Microwave Photonics in 2007. He has authored or coauthored over 320 papers, including over 180 papers in refereed journals and over 140 papers in conference proceeding. He is an Associate Editor of the *International Journal of Microwave and Optical Technology*. His research has focused on microwave photonics, which includes all-optical microwave signal processing, photonic generation of microwave, millimeter-wave and terahertz, radio-over-fiber, ultra-wideband (UWB) over fiber, FBGs for microwave photonics applications, and optically controlled phased-array antenna. His research interests also include fiber lasers, fiber-optic sensors, and bio-photonics.

Dr. Yao is a Registered Professional Engineer of the Province of Ontario. He is a Fellow of the Optical Society of America. He is a Senior Member of the IEEE Photonics Society and the IEEE Microwave Theory and Techniques Society (IEEE MTT-S). He is on the Editorial Board of the IEEE TRANSACTIONS ON MICROWAVE THEORY AND TECHNIQUES. He was the recipient of the 2005 International Creative Research Award of the University of Ottawa, the 2007 George S. Glinski Award for Excellence in Research, and a 2008 Natural Sciences and Engineering Research Council of Canada (NSERC) Discovery Accelerator Supplements Award.